Host Factors Influencing the Preferential Localization of Sterically Stabilized Liposomes in *Klebsiella pneumoniae*-Infected Rat Lung Tissue

R. M. Schiffelers,[1,2,3] **G. Storm,**[2] **and I. A. J. M. Bakker-Woudenberg**[1]

Purpose. To gain insight into the host factors influencing liposome localization at sites of bacterial infection.

Methods. In a unilateral *Klebsiella pneumoniae* pneumonia rat model, capillary permeability and number of circulating leukocytes was quantified and related to the degree of liposome target localization.

Results. Liposome localization was highest in the hemorrhagic zone of infection, a zone characterized by markedly increased capillary permeability and high bacterial numbers. Both liposome localization and capillary permeability correlated positively with severity of infection. Lung instillation of other inflammatory stimuli, such as lipopolysaccharide or 0.1 M HCl inducing increased capillary permeability, also promoted liposome localization. As liposomal target localization in leukopenic rats was similar to that in immunocompetent rats, contribution of circulating leukocytes seems limited. Intrapulmonary distribution of liposomes shows that leukocytes at the target site are involved in liposome uptake after extravasation.

Conclusions. Increased capillary permeability plays a crucial role in liposome localization at the infected site, whereas contribution of leukocytes is limited. These results suggest inflammatory conditions that could benefit from liposomal drug delivery. The involvement of leukocytes in liposome uptake at the target site could be important information in the selection of appropriate drugs.

KEY WORDS: inflammatory response; *Klebsiella pneumoniae*; leukocytes; liposomes; pneumonia; rat.

INTRODUCTION

Targeted delivery of antibiotics may improve antibacterial therapy by increasing the concentration of the drug at the site of infection. Liposomes have been investigated as targeted drug carriers for this purpose. The avid uptake of conventional liposomes after intravenous administration, by the cells of the mononuclear phagocyte system (MPS), has been employed to deliver substantial amounts of antibiotics selectively to the cells of this system (1–2). However, the prompt uptake by MPS-cells strongly limits the chance that conventional liposomes will interact with sites of infections located outside the major MPS-organs.

The development of liposomes coated with poly(ethylene) glycol (PEG), also known as sterically stabilized liposomes (SSL), potentially permits liposomal drug delivery to tissues beyond the MPS-cells (3–6). SSL display a reduced affinity for the MPS, compared to liposomes lacking the PEG-coating. It is believed that the PEG-coating reduces the interaction of opsonins with the SSL surface, thereby reducing MPS recognition and uptake. As a result SSL display a prolonged circulation time. In experimental models representing a variety of inflammatory and infectious foci outside the MPS, substantial SSL localization at the site of infection has been demonstrated. The presence of an infectious process is essential as SSL localization in uninfected controls is limited (7–13). Previous reports have suggested that presence of the long circulation property is also essential to achieve significant localization at the target site (5–6,14). In addition, SSL-encapsulated gentamicin showed improved efficacy compared to the free drug in a rat model of *Klebsiella pneumoniae* pneumonia (15). These data warrant further investigations on SSL as carriers of antibiotics to sites of infection beyond the cells of the MPS.

At present, limited information is available on the host factors that are responsible for the selective SSL localization at inflammatory sites, compared to non-infected control organs. It has been suggested that the increased capillary permeability at inflammatory foci allows SSL to extravasate (14). Besides, the infiltration of inflammatory cells may actively or passively promote SSL localization, either by taking up liposomes in the circulation and subsequent infiltration into the inflamed tissue, or by facilitating liposome extravasation as a result of leukocyte-mediated tissue inury (16).

The present study was designed to gain more insight into the mechanism of localization of SSL at sites of infection. In a rat model of a unilateral pneumonia caused by *Klebsiella pneumoniae* the requirement of increased capillary permeability for achieving SSL localization was investigated by correlating the extent of capillary permeability to the degree of SSL localization. The correlation was also studied after lung-instillation of other inflammatory stimuli (lipopolysaccharide (LPS) and 0.1 M HCl). The involvement of leukocytes in SSL extravasation was investigated by leukocyte depletion. Micrsocopic visualization of colloidal-gold labeled SSL was performed to obtain information on the intrapulmonary localization of SSL after extravasation in the infected tissue.

MATERIALS AND METHODS

Animals

RP/AEur/RijHsd strain albino rats, with a specified pathogen-free status (18–25 weeks of age, weighing 185–225 g) (Harlan, Horst, The Netherlands), were used in the experiments. Rats were housed individually with free access to sterilized water and SRMA chow (Hope Farms, Woerden, The Netherlands).

Bacterial Inoculation of the Left Lung

Bacteria were inoculated in the left lung as described previously (17). Briefly, rats were anaesthetized by an intra-

[1] Department of Medical Microbiology & Infectious Diseases, Erasmus University Medical Center Rotterdam (EMCR), PO Box 1738, 3000 DR Rotterdam, The Netherlands.

[2] Department of Pharmaceutics, Utrecht Institute for Pharmaceutical Sciences (UIPS), Utrecht University, PO Box 80082, 3508 TB Utrecht, The Netherlands.

[3] To whom correspondence should be addressed. (e-mail: schiffelers@kmic.fgg.eur.nl)

ABBREVIATIONS: C, consolidated zone; EI, early-infected zone; H, hemorrhagic zone; LL, (infected) left lung; LPS, lippolysaccharide; MPS, mononuclear phagocyte system; PEG, poly(ethylene) glycol; RL, (uninfected) right lung; SSL, sterically stabilized liposome.

muscular injection of fluanisone and fentanyl citrate (Janssen Animal Health, Saunderton, UK) followed by an intraperitoneal injection of pentobarbital (Sanofi Santé b.v., Maassluis, The Netherlands). The left primary bronchus was subsequently intubated and 0.02 ml of a saline suspension containing the indicated number of *K. pneumoniae* (ATCC 43816, capsular serotype 2) was inoculated in the lower left lung lobe. Following the inoculation, rats received an intramuscular injection of nalorphine bromide as an anesthetic antagonist (Onderlinge Pharmaceutische Groothandel, Utrecht, The Netherlands).

When indicated, leukopenia was effectuated by intraperitoneal injection of 60 mg/kg cyclophosphamide (Sigma, St. Louis, MO) every 4 days starting at 5 days before bacterial inoculation, according to Leenders *et al.* (18). Leukopenia was ascertained by measuring leukocyte counts in fresh blood samples, obtained by retro-orbital bleeding just before SSL injection. Leukocytes were counted on a Cobas Minos Stex (Roche Haematology, Montpellier, France) using Minotrol™ 16 standards (Roche Haematology, Montpellier, France) to verify proper functioning of the instrument.

Instillation of Other Inflammatory Stimuli in the Left Lung

Rats were anesthetized and intubated as described above. 0.02 ml of a saline solution containing 2 mg LPS (from *Escherichia coli,* serotype 0111:B4 (Sigma, St. Louis, MO)) or 0.1 ml aqueous 0.1 M HCl (Fluka, Buchs, Switzerland) were instilled in the lower left lung lobe. Nalorphine bromide was injected as an anesthetic antagonist.

SSL Preparation

SSL were prepared as described previously (13,15). In brief, appropriate amounts of partially hydrogenated egg phosphatidylcholine (PHEPC) (Asahi Chemical Industry Co. Ltd., Ibarakiken, Japan), cholesterol (Chol) (Sigma Chemical Co., St. Louis, MO), and 1,2-distearoyl-sn-glycero-3-phosphoethanolamine-N-[polyethylene glycol-2000] (PEG-DSPE) (Avanti polar lipids, Alabaster, Alabama) in a molar ratio of 1.85: 1.00:0.15, respectively, were dissolved in chloroform:methanol in a round bottom flask, followed by evaporation of the solvent in a rotary evaporator. The lipid mixture was dried under nitrogen for 15 min, dissolved in 2-methyl-2-propanol (Sigma Chemical Co., St. Louis, MO) and freeze-dried overnight. The resulting lipid film was hydrated for 2 h in Hepes/NaCl buffer, pH 7.4 (10 mM N-[2-hydroxy ethyl] piperazine-N′-ethane sulfonic acid (Hepes) (Sigma Chemical Co., St. Louis, MO) and 135 mM NaCl (Merck, Darmstadt, Germany) containing 5 mM of the chelator deferoxamine mesylate (Desferal®) (Novartis, Basel, Switzerland). SSL were sized by subjecting the hydrated lipid dispersion to a sonication procedure for 8 min with an amplitude of 8 µ using a 9.5 mm probe in an MSE Soniprep 150 (Sanyo Gallenkamp PLC, Leicester, UK).

Radiolabeling of Liposomes

Non-encapsulated deferoxamine was removed by gel filtration of the SSL over a Sephadex G-50 column (Pharmacia, Uppsalla, Sweden) using Hepes/NaCl buffer as an eluens. The SSL were subsequently concentrated via ultracentrifugation at 365,000 × g for 2 h at 4°C in a Beckman ultracentrifuge L-70 (Beckman, Palo Alto, CA). SSL were labeled with ^{67}Ga according to Gabizon *et al.* (19). ^{67}Ga-citrate (1 mCi/ml) (Mallinckrodt Medical, Petten, The Netherlands), diluted 1:10 in aqueous 5 mg/ml 8-hydroxyquinone (Sigma Chemical Co., St. Louis, MO), was incubated for 1 h at 52°C to obtain ^{67}Ga-oxine. 1 ml of this mixture was added per 1000 µmol total lipid (TL) of SSL. ^{67}Ga-oxine can pass the liposomal membrane and has a high affinity for the encapsulated chelator deferoxamine, with the result that the radioactive label becomes entrapped. ^{67}Ga-deferoxamine is a suitable label for studying intact liposomes in the circulation because it is excreted rapidly via the kidneys in case it leaks from the liposomes (19). Unencapsulated ^{67}Ga was removed by gel filtration and radiolabeled SSL were concentrated by ultracentrifugation. Resulting specific activity was approximately 10^5 cpm/µmol TL.

SSL Characterization

Particle size distribution of the SSL was measured using dynamic light scattering, detected at an angle of 90° to the laser beam on a Malvern700 System (Malvern Instruments Ltd., Malvern, UK). The polydispersity of the liposome population is reported by the system as a value between 0 and 1. A reported value of 1 indicates large variations in particle sizes, whereas a value of 0 indicates a complete monodisperse system. For all SSL preparations used in the experiments, the mean liposomal size was approximately 100 nm and the polydispersity was below 0.3. Phosphate concentration was determined colorimetrically according to Bartlett (20).

Bacterial Counts

At indicated time points after bacterial inoculation, rats were sacrificed by CO_2 inhalation, since this form of euthanasia does not affect bacterial counts (unpublished observations). The right and left lung were excised and kept on ice and the left lung was divided into the three distinct zones of the lobar pneumonia: the early infected, hemorrhagic, and consolidated zone. Lung (zones) were homogenized in 20 ml of phosphate buffered saline (4°C), appropriate dilutions were cultured (overnight, 37°C) on tryptone soy agar plates (Oxoid, Basingstoke, UK) and bacterial colonies were counted.

Evan's Blue Dye Extravasation

Evan's blue dye extravasation is a measure for the capillary permeability (21–22) and was determined as described previously by Zhang *et al.* (21). A saline suspension of Evan's blue dye (40 mg/kg) (Merck, Darmstadt, Germany) was injected in the tail vein at indicated time points after inoculation of the left lung. Rats were sacrificed 24 h later. A blood sample was taken via retro-orbital puncture, the lungs were excised and, when indicated, the left lung was divided into the three distinct zones of the lobar pneumonia. Blood sample volume was measured and the right lung and the three zones of the left lung were weighed and put in 7 ml of formamide (Sigma, St. Louis, MO) to extract the dye. Absorbance was measured on an LKB Ultrospec Plus spectrometer (Pharmacia, Uppsalla, Sweden) at a wavelength of 623 nm. Standards (0–30 µg Evan's blue/ml) were also dissolved in formamide.

Corrections were made for the amount of Evan's blue present in the blood (see SSL localization).

Lung Wet-to-Dry Weight Ratio

Another measure of capillary permeability is the wet-to-dry weight ratio (23). Animals were sacrificed at 64 h after bacterial inoculation, the lungs were excised and left and right lung weight was determined. Lungs were subsequently dried in a stove for 3 days at 70°C, the dry weight of the lungs was determined and the wet-to-dry weight ratio was calculated.

SSL Localization

SSL (75 μmol TL/kg) were administered via the tail vein 24 h before the rats were sacrificed by an i.v. overdose of pentobarbital, at indicated time points after inoculation of the left lung. A blood sample was taken via retro-orbital puncture, lungs were excised and, when indicated, the left lung was divided into the three distinct zones of a lobar pneumonia. The right lung and the three zones of the left lung were weighed and radioactivity was counted in a Minaxi auto-gamma 5000 gamma counter (Packard Instrument Company, Meriden, CT) to assess the degree of localization of the SSL. Blood content of the tissues was determined in independent experiments with ^{111}In-oxine labeled syngeneic erythrocytes, as described by Kurantsin-Mills *et al.* (24). Labeled erythrocytes were injected 10 min before the animals were sacrificed. Assuming that all erythrocytes are still present in the circulation, the dilution factor of the label allows determination of total blood volume and the blood content of the tissues of interest. Blood content values were used to correct for the contribution of labeled SSL in the circulation to total tissue radioactivity.

Blood Cell-Associated SSL

To determine the amount of cell-associated SSL in the circulation, blood samples were obtained from infected animals via retro-orbital bleeding in heparanized tubes at indicated time points after injection of radioactively labeled SSL. Blood cells (0.5 ml sample) were washed three times in 50 ml PBS (4°C) by centrifugation at $1500 \times g$ for 10 min (Hettich Rotanta, Germany). Radioactivity of pellet and supernatants was counted as described above.

Colloidal Gold-Labeling of SSL

Colloidal gold-labeled SSL were prepared as described by Daemen *et al.* (25). Briefly, the lipid film was prepared as described above. A 1.1% (w/v) aqueous solution of $AuCl_2$ (Sigma, St. Louis, MO) was four-fold diluted with sodium citrate (28 mM)/ potassium carbonate (7 mM) buffer, filtered (0.2 μm), and used to hydrate the lipid film at 4°C. SSL were prepared by multiple extrusion of the hydrated lipids through two stacked 100 nm membranes (Nuclepore, Pleasanton, CA). The resulting yellow SSL suspension was placed at 37°C, after which the color of the suspension turned purple. Unencapsulated colloidal gold was removed by gel filtration of the SSL suspension over a Sephacryl SF S1000 column (Pharmacia, Uppsalla, Sweden) using Hepes/NaCl buffer as the eluens.

Localization of Colloidal-Gold Labeled SSL

Colloidal-gold labeled SSL (approx. 5 μmol TL/kg) were injected at 40 h after bacterial inoculation of the left lung. 24 h after injection both right and left lung were excised, washed in three changes of 2.5% buffered formaldehyde (Merck, Darmstadt, Germany), fixed in 10% buffered formaldehyde and embedded in paraffin. 5 μm sections were cut on a microtome and mounted on slides. Sections were deparaffinized in two changes of xylene and hydrated. Next, colloidal gold was silver-enhanced using a silver-enhancement kit (Sigma, St. Louis, MO) according to the manufacturer's instructions. Eosin/haematoxylin was applied as a counterstain, when indicated.

For the immunohistochemical staining procedure, slides were deparaffinised and hydrated as described above. Endogenous peroxidase activity was blocked by incubation of slides for 10 min in 3% H_2O_2 (Merck, Darmstadt, Germany) in methanol (Fluka, Buchs, Switzerland) followed by rinsing with PBS. Slides were incubated with 5% goat serum for 30 min. Then 0.4 μg/ml of mouse anti-rat CD43 (Pharmingen, San Diego, CA) was applied and slides were incubated overnight at 4°C in a humid container. Slides were rinsed in 3 changes of PBS and the secondary polyclonal horseradish peroxidase conjugated goat anti-mouse IgG (10 μg/ml) (Pharmingen, San Diego, CA) was added, incubated for 30 min at room temperature and rinsed in 3 changes of PBS. Peroxidase activity was detected using the 3-amino-9-ethylcarbazole kit (Sigma, St. Louis, MO) according to manufacturers instructions.

Statistical Analysis

Indicated statistical analyses were performed using SPSS for Windows software release 7.5.2 (Statistical Product & Service Solutions Inc., Chicago, IL).

RESULTS

Characteristics of the Lobar *K. pneumoniae* Pneumonia

At 64 h after inoculation of the left lung of the rats with 10^6 *K. pneumoniae* a lobar pneumonia had developed (Fig. 1). Three zones characteristic for this type of pneumonia can be clearly distinguished. The consolidated zone (C) is the lower part of the lung where the bacterial inoculum was deposited and the infectious process started. As the active infection gradually moves upward, the consolidated area is characterized by gray hepatization. Microscopic evaluation (data not shown) indicated disintegration of alveolar walls, cellular debris, limited blood flow, and the deposition of connective tissue. The hemorrhagic zone (H) is the active area of the infection featured by a dark red appearance. Microscopic observations (data not shown) indicate the presence of edema fluid, a large number of bacteria, infiltrating leukocytes, and hemorrhagic areas. The early-infected zone (EI) appears macroscopically as normal lung tissue, however, microscopic evaluation (data not shown) reveals the presence of bacteria and leukocytes indicates the early involvement in the infectious process. Because the three zones of the lobar pneumonia can be clearly distinguished at 64 h after inoculation and these zones showed limited variation in size and macroscopic appearance between animals, this time-point was chosen to
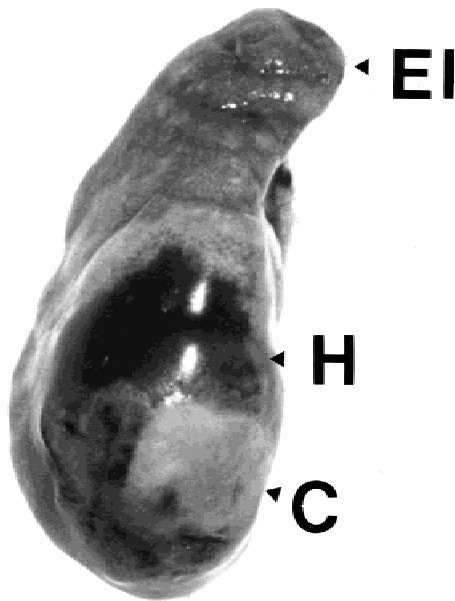
Fig. 1. The consolidated (C), hemorrhagic (H), and early infected (EI) zone of an acute lobar pneumonia in the left lung of a rat at 64 h after inoculation of the left lung with 10^6 K. pneumoniae.

Fig. 2. Localization of bacteria (A), Evan's blue (B), and ^{67}Ga-labeled SSL (C) in right lung (RL) and infected left lung (LL) (closed bars) (n = 6, mean ± standard deviation). Localization within the LL in the consolidated (C), hemorrhagic (H), and early infected (EI) zone of the lobar pneumonia (open bars) (n = 6, mean ± standard deviation). $*P <0.05$, $**P <0.01$, $***P <0.001$, left lung compared to right lung (paired t test), consolidated zone and early infected zone each compared to hemorrhagic zone (repeated measures ANOVA corrected for multiple comparisons by the Bonferroni method). Tissues were dissected at 64 h after inoculation of the left lung with 10^6 K. pneumoniae, at 24 h after injection of liposomes and Evan's blue.

examine bacterial counts, capillary permeability, and SSL localization.

As expected, significantly higher bacterial numbers were observed in the infected left lung (LL) per gram organ weight compared to the uninfected right lung (RL) at 64 h after inoculation. The distribution of the bacteria over the three different zones of the lobar pneumonia shows that the number of bacteria was significantly higher in zone H of the pneumonia compared to C and EI (Fig. 2A). The localization of a marker for capillary permeability–Evan's blue–shows a similar pattern at 24 h after injection (Fig. 2B). A significantly higher level of Evan's blue was seen in the infected left lung compared to the contralateral non-infected right lung. The level of Evan's blue in the right lung was comparable to the levels measured in lungs of uninfected rats (data not shown). Within the infected lung a significantly higher level of Evan's blue was present in zone H compared to C and EI. Another measure for capillary permeability is the tissue wet-to-dry weight ratio. The wet-to-dry weight ratio was lower for the uninfected right lung (4.81 ± 0.05) compared to the infected left lung (5.84 ± 0.06) (mean ± standard deviation, n = 10) ($P < 0.0001$, paired t test). Localization of ^{67}Ga-labeled SSL shows the same profile at 24 h after injection (Fig. 2C). Significantly higher levels were seen in the infected left lung compared to the right lung. Within the infected lung the highest level of SSL localization was seen in zone H compared to C and EI.

Effect of Increase in Inoculum Size on Localization of SSL and Evan's Blue

To test whether the severity of infection has an effect on capillary permeability and SSL localization, three different inocula of K. pneumoniae were applied and compared to sterile buffer-inoculated animals (Fig. 3). Tissues were dissected at 48 h after inoculation as the highest inoculum already in-
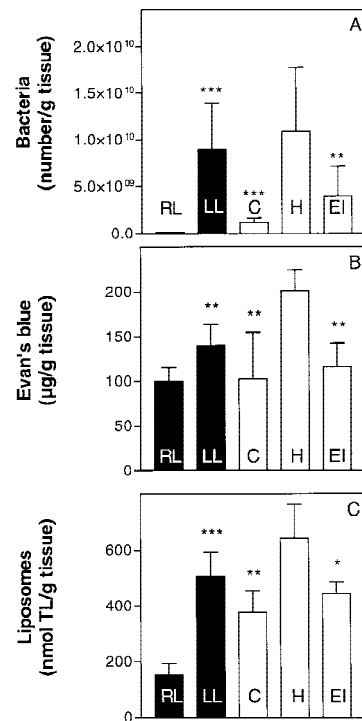
duced mortality at 64 h after inoculation. Evan's blue dye localization and ^{67}Ga-labeled SSL localization measured at 24 h after injection, increased with an increasing inoculum (r = 0.91, $P <0.0001$, r = 0.91, $P <0.0001$, both Spearman's correlation test).
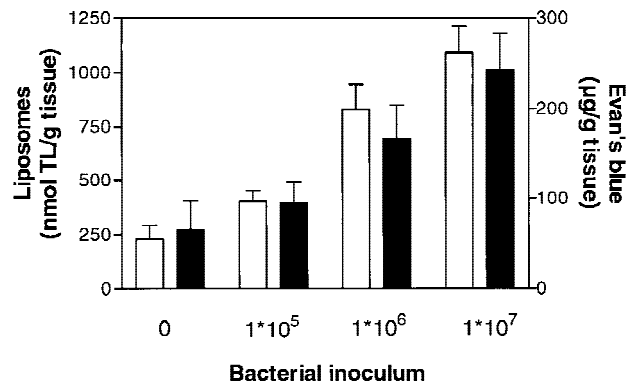

Fig. 3. Effect of increasing K. pneumoniae inoculum on degree of localization of SSL (open bars) and Evan's blue (closed bars) in the inoculated left lung (LL) (n = 6, mean ± standard deviation). Tissues were dissected at 48 h after bacterial inoculation of the left lung, at 24 h after injection of liposomes and Evan's blue.

Effect of Local Administration of LPS and HCl on Left Lung Localization of SSL and Evan's Blue

LPS, a component of the Gram-negative bacterial cell wall, has been shown to increase capillary permeability in lung tissue after local administration (26). To test whether an increase in capillary permeability induced by LPS in the absence of living bacteria also produces increased ^{67}Ga-labeled SSL localization, 2 mg LPS was inoculated in the left lung. After instillation of the LPS a significantly increased localization of ^{67}Ga-labeled SSL and Evan's blue in the lung was noted at 24 h after injection (Fig. 4). Similarly, inoculation of the left lung with 0.1 ml 0.1 M HCl, a model for adult respiratory distress syndrome featured by an increased capillary permeability (23), resulted in an increased localization of ^{67}Ga-labeled SSL and Evan's blue at 24 h after injection (Fig. 4).

Effect of Leukocytes on Localization of SSL

To investigate whether SSL are taken up by circulating leukocytes, ^{67}Ga-labeled SSL were injected i.v. Blood samples were washed three times in PBS by centrifugation. The amount of cell-associated radioactivity was determined.
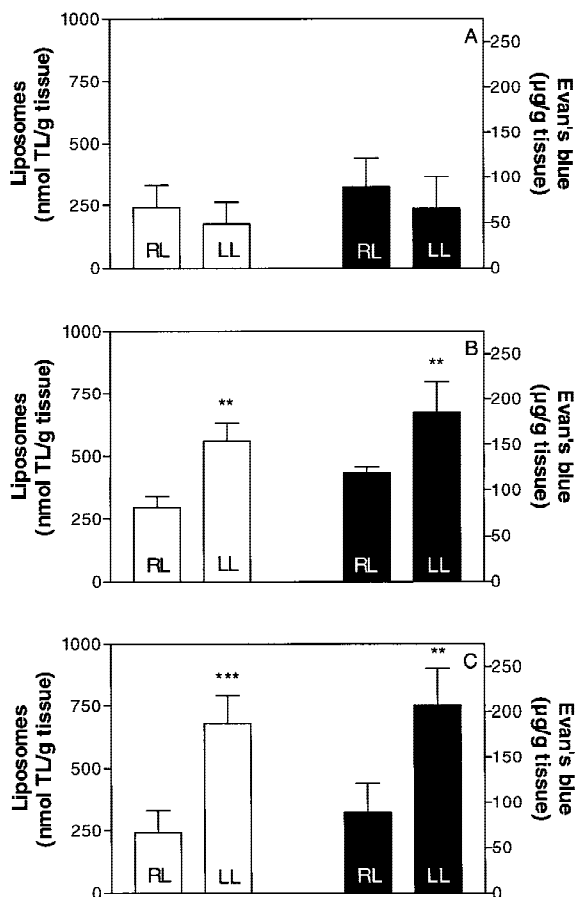
In blood samples obtained at 1 h, 4 h, and 24 h after SSL injection $0.28 \pm 0.12\%$, $0.35 \pm 0.16\%$, and $0.17 \pm 0.08\%$ of the recovered radioactivity was pelletable with the blood cell fraction, respectively (mean ± standard deviation, n = 3).

To establish whether extravasation of inflammatory cells is a key factor contributing to SSL localization in the left lung, the number of leukocytes in the circulation was reduced by i.p. injections of cyclophosphamide. As a result of the cyclophosphamide treatment, the number of leukocytes in the blood was reduced 6-fold from $5.8 \times 10^9 \pm 1 \times 10^9$ for the buffer treated controls to $1 \times 10^9 \pm 8 \times 10^8$ for the cyclophosphamide treated rats (mean ± standard deviation, n = 3) ($P <0.01$, unpaired t test). Tissues were dissected at 48 h after inoculation as the infection produced mortality in the leukopenic animals already at 64 h after inoculation. At 24 h after injection of ^{67}Ga-labeled SSL, SSL localization in the infected left lung of either leukopenic animals or animals with an intact host defense was significantly higher compared to ^{67}Ga-labeled SSL localization in the lungs of uninfected animals (Fig. 5). Cyclophosphamide treatment did not result in a significant difference in the degree of ^{67}Ga-labeled SSL localization in infected animals.

Microscopic Evaluation of Colloidal Gold-Labeled SSL Within the Infected Site

Localization of SSL in infected left lung and uninfected right lung tissue was visualized using silver-enhancement of colloidal gold-labeled SSL. Figure 6A and B show dense clusters of silver-enhanced colloidal gold in the connective tissue surrounding the primary bronchus and major bronchioles of the infected left lung. These clusters were not observed in the uninfected right lung. Magnification of these clusters show that the silver-enhanced colloidal-gold is present in mononuclear cells (Fig. 6C). These cells stained positive immuno-
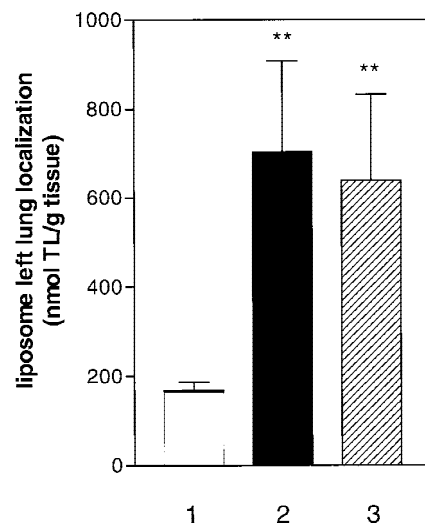
Fig. 4. Localization of liposomes (open bars) and Evan's blue (closed bars) in right lung (RL) and left lung (LL) of rats inoculated with buffer (A), 2 mg LPS per left lung (B), and 0.1 ml 0.1 M HCl per left lung (C). Liposomes and Evan's blue were injected 15 min after inoculation. Tissues were dissected at 24 h after injection of liposomes and Evan's blue. (n = 6, mean ± standard deviation). *$P <0.05$, **$P <0.01$, ***$P <0.001$ compared to right lung (paired t test).

Fig. 5. Localization of liposomes in the left lung of uninfected rats with intact host defense (1), infected rats with intact host defense (2), and infected leukopenic rats (3) (n = 6, mean ± standard deviation). Tissues were dissected at 48 h after inoculation of the left lung inoculated with 10^6 *K. pneumoniae,* at 24 h after injection of liposomes and Evan's blue. **$P <0.01$ infected rats compared to uninfected rats. No significant differences were noted between leukopenic infected rats and infected rats with an intact host defense (ANOVA corrected for multiple comparisons by the Bonferroni method).

histochemically for CD43 (Fig. 6D). One aspect of SSL local-ization that could only be clearly visualized in slides unstained or with just a very light counterstain is the presence of SSL in and around alveolar capillaries. Micrographs show silver granula in and around the capillaries in the alveolar walls, most prominent in the hemorrhagic zone of infected left lung tissue (Fig. 6E,F). Silver granula were not seen surrounding capillaries or alveolar walls in the uninfected right lung tissue.
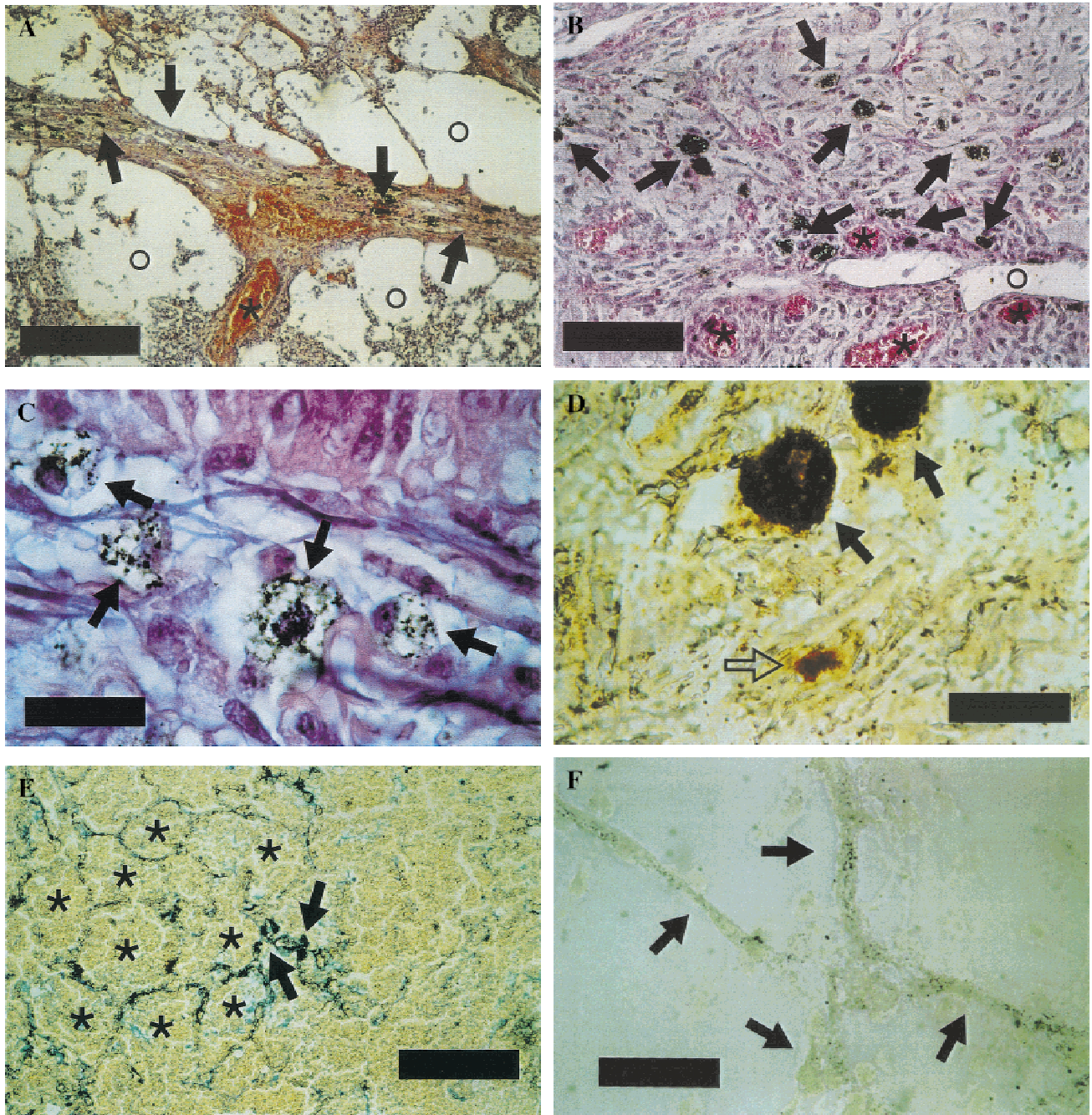

Fig. 6. Localization of colloidal gold-labeled liposomes in infected left lung tissue. A. Presence of silver-enhanced colloidal gold-labeled SSL in large clusters (arrows) in the connective tissue surrounding the large bronchioles and blood vessels (asterisk). Inflamed alveolar spaces with high numbers of leukocytes surround the connective tissue (circles). Counterstain haematoxylin/eosin. Bar = 1125 μm. B. Magnification of clusters, as shown in A. Separate silver-enhanced colloidal gold-labeled clusters (arrows) can be clearly distinguished from surrounding tissue, in which a bronchiolar lumen (circle) and blood vessels (asterisks) are identified. Counterstain haematoxylin/eosin. Bar = 450 μm. C. Magnification of clusters, as shown in B. Clusters appear intracellular silver-enhanced colloidal-gold in a mononuclear cell. Bar = 45 μm. D. Positive immunohistochemical staining for CD43 of cells containing silver-enhanced colloidal gold-labeled SSL (closed arrows). Not all positively stained leukocytes show colloidal-gold accumulation (open arrow). Peroxidase activity was detected by 3 amino-9-ethylcarbazole. Bar = 45 μm. E. Localization of silver-enhanced colloidal gold-labeled SSL in and around alveolar capillaries in the alveolar walls, surrounding the alveolar spaces (asterisks) in a hemorrhagic area of the infected lung. Clustered silver-enhanced colloidal-gold may indicate cellular uptake (arrows). Lightly counterstained with haematoxylin/eosin. Bar = 450 μm. F. Localization of silver-enhanced colloidal gold-labeled SSL (arrows) in and around alveolar capillaries in the alveolar walls. No counterstain. Bar = 45 μm.

DISCUSSION

Preferential localization of SSL at sites of infection or inflammation that have developed outside the MPS has been reported by a number of investigators (7–13). Which host factors contribute to selective extravasation of SSL at infectious or inflammatory foci is not clear. In the present study, the involvement of increased capillary permeability and the role of inflammatory cells in the selective localization of SSL in bacterially infected lungs was studied in a rat model of unilateral pneumonia caused by *K. pneumoniae*.

Three distinct zones of infection characterize the lobar unilateral *K. pneumoniae* pneumonia: the early infected, hemorrhagic, and consolidated zone. When the distribution of bacteria was studied at 64 h after inoculation, a higher number of bacteria was present in the inoculated left lung compared to the right lung. Within the infected left lung, the highest number of bacteria is present in the active hemorrhagic zone of the infection compared to the consolidated zone and early-infected zone. It is shown that the high number of bacteria in the hemorrhagic zone of the infected lung correlates with a pronounced inflammatory response, featured by a significantly increased capillary permeability as reflected by Evan's blue dye levels and lung wet-to-dry weight ratio. Furthermore, by raising the bacterial inoculum and thereby aggravating the severity of the infection, the increase in capillary permeability is enlarged. The increase in capillary permeability was invariably seen along with a proportional increase in SSL localization illustrating that capillary permeability is an important determinant for SSL extravasation. The observed correlation between capillary permeability and SSL extravasation is in line with studies showing preferential accumulation of SSL in tumor tissue, possessing angiogenic blood vessels exhibiting increased permeability, as has been reviewed (4–6). It also supports the observation of Klimuk *et al.* that increase in vascular permeability and liposome localization occur simultaneously in a model of delayed type hypersensitivity (8).

Increased capillary permeability has been described after intratracheal administration of LPS and HCl in rats (23,26). Also in our experiments, both inflammatory stimuli promoted an increase in capillary permeability as well as SSL localization. Apparently, the nature of the inflammatory stimulus is not important for SSL localization as long as a sufficient increase in capillary permeability is effectuated. Preferential SSL localization at the target site has been demonstrated in a wide variety of models of experimental inflammation and infection, including pathology as a result of administration of guinea-pig spinal cord (allergic encephalomyelitis) (7), 2,4-dinitrofluorobenzene (delayed type hypersensitivity) (8), trinitrobenzene sulfonic acid (acute colitis) (9), sodium-morrhuate and *Staphylococcus aureus* (osteomyelitis) (10), *Mycobacterium butyricum* (adjuvant arthritis) (11), turpentine or *Staphylococcus aureus* (focal infection or inflammation) (12), and *K. pneumoniae* (unilateral pneumonia) (13). These findings strongly suggest that the etiology or location of the pathological process is not decisive for achieving SSL localization. Instead, increased capillary permeability, as part of the inflammatory response is likely to be the decisive parameter.

Previous studies in models of hypersensitivity, colitis, and encephalomyelitis have reported preferential SSL localization

as well as leukocyte influx at the site of inflammation (7–9). Also in the present model, the inflammatory response involves leukocyte infiltration. It has been suggested that there is a correlation between SSL and leukocyte localization (14). In the present study, it is shown that the amount of cell-associated SSL-encapsulated radioactivity in the circulation is negligible. In addition, a 6-fold reduction of the number of leukocytes in the circulation by cyclophosphamide injections did not result in a reduced degree of SSL localization in the infected lung compared to rats with normal levels of leukocytes. In addition, Dams *et al.* showed that SSL still localized preferentially at sites of infection in granulocytopenic rats (27). These results strongly suggest that the contribution of circulating leukocytes to SSL localization at the site of infection is limited. An important implication would be that liposomal drug delivery could also be beneficial to leukopenic patients. These patients are highly susceptible to infections that are difficult to treat as a result of a reduced support by the host defense (28).

Microscopic evaluation of silver-enhanced colloidal gold-labeled SSL in lung tissue showed that SSL could be visualized principally in the infected left lung. In the left lung, SSL were present in dense clusters in the connective tissue surrounding the primary bronchus and main bronchioles. These clusters appeared to be uptake by CD43-positive mononuclear leukocytes. SSL were also seen surrounding capillaries in alveolar walls, especially in the hemorrhagic zone of infection, supporting the observation that increased capillary permeability allows liposome extravasation. To our knowledge, the localization of SSL around capillaries and liposome uptake at the site of bacterial infection by leukocytes has not been demonstrated before. Our results are in line with studies obtained in other models showing that SSL are taken up by inflammatory cells present at the inflamed tissue. In the FSN mouse (having a gene mutation producing inflammatory lesions resembling psoriasis) (29), in mice having been injected with substance P (30), and in mice overexpressing the HIV *tat* gene showing lesions resembling Kaposi's sarcoma (31), selective SSL localization at the target site was demonstrated together with uptake of colloidal gold labeled SSL by phagocytic cells. It is tempting to speculate that phagocytic cells at the pathological site are involved in the processing of SSL and release of encapsulated agents. Still, the quantitative contribution of SSL uptake by local phagocytes to the fate of SSL localizing within the infected area remains unclear.

In conclusion, our observations indicate that the selectivity of SSL localization is a result of the local inflammatory response, as the locally increased capillary permeability seems decisive for SSL localization. The localization process appears independent of the nature of the inflammatory stimulus and number of circulating leukocytes. Microscopic observations indicate that phagocytes are to a certain extent involved in SSL uptake at the site of infection. In addition, extravasation of liposomes is observed in the alveolar walls. Further elucidation of the processes that determine the fate of SSL after target site localization, may help to design SSL-antibiotic formulations with increased antibacterial activity.

ACKNOWLEDGMENTS

Kwast (dept. of Pathology, Erasmus *university* Medical Center Rotterdam) is thanked for helpful comments on colloidal-gold labeled liposome localization.

REFERENCES

1. A. J. Schroit, J. Madsen, and R. Nayar. R. Liposome-cell interactions: *In vitro* discrimination of uptake mechanism and *in vivo* targeting strategies to mononuclear phagocytes. *Chem. Phys. Lipids* **40**:373–393 (1986).
2. R. Kirsh and G. Poste. Liposome targeting to macrophages: Opportunities for treatment of infectious diseases. *Adv. Exp. Med.* **202**:171–184 (1986).
3. G. Storm and D. J. A. Crommelin. Liposomes-Quo vadis? *Pharm. Sci. Technol. Today* **1**:19–31 (1998).
4. M. C. Woodle, M. S. Newman, and P. K. Working. Biological properties of sterically stabilized liposomes. In D. Lasic and F. J. Martin (eds.), *Stealth Liposomes*, CRC Press, Boca Raton, 1995 pp. 103–117.
5. G. Storm and M. C. Woodle. Long circulating liposomes: from concept to clinical reality. In M. C. Woodle and G. Storm (eds.), *Long Circulating Liposomes: Old Drugs, New Therapeutics*, Springer Verlag, Germany, 1998 pp. 3–16.
6. T. M. Allen. Liposomes: Opportunities in drug delivery. *Drugs* **54S1**:8–14, (1997).
7. V. Rousseau, B. Denizot, J. J. Le Jeune, and P. Jallet. Early detection of liposome brain localization in rat experimental allergic encephalomyelitis. *Exp. Brain Res.* **125**:255–264 (1999).
8. S. K. Klimuk, S. C. Semple, P. Scherrer, and M. J. Hope. Contact hypersensitivity: A simple model for the characterization of disease-site targeting by liposomes. *Biochim. Biophys. Acta* **1417**:191–201 (1999).
9. E. T. Dams, W. J. Oyen, and O. C. Boerman. Technetium-99m-labeled liposomes to image experimental colitis in rabbits: Comparison with technetium-99m-HMPAO-granulocytes and technetium-99m-HYNIC-IgG. *J. Nucl. Med.* **39**:2172–2178 (1998).
10. V. Awasthi, B. Goins, R. Klipper, R. Loredo, D. Korvick, and W. T. Phillips. Imaging experimental osteomyelitis using radiolabeled liposomes. *J. Nucl. Med.* **39**:1089–1094 (1998).
11. M. L. Corvo, O. C. Boerman, W. J. Oyen, L. van Bloois, M. E. Cruz, D. J. A. Crommelin, and G. Storm. Intravenous administration of superoxide dismutase entrapped in long circulating liposomes. II. *In vivo* fate in a rat model of adjuvant arthritis. *Biochim. Biophys. Acta* **1419**:325–334 (1999).
12. W. J. Oyen, O. C. Boerman, and G. Storm. Detecting infection and inflammation with technetium-99m-labeled Stealth liposomes. *J. Nucl. Med.* **37**:1392–1397 (1996).
13. I. A. J. M. Bakker-Woudenberg, A. F. Lokerse, M. T. ten Kate, J. W. Mouton, M. C. Woodle, and G. Storm. Liposomes with prolonged blood circulation and selective localization in *Klebsiella pneumoniae*-infected lung tissue. *J. Inf. Dis.* **168**:164–171 (1993).
14. W. J. Oyen, O. C. Boerman, C. J. van der Laken, R. A. Claessens, J. W. van der Meer, and F. H. Corstens. The uptake mechanisms of inflammation- and infection-localizing agents. *Eur. J. Nucl. Med.* **23**:459–465 (1996).
15. I. A. J. M. Bakker-Woudenberg, M. T. ten Kate, L. E. T. Stearne-Cullen, and M. C. Woodle. Efficacy of gentamicin or ceftazidime entrapped in liposomes with prolonged blood circulation and enhanced localization in *Klebsiella pneumoniae*-infected lung tissue. *J. Inf. Dis.* **171**:938–947 (1995).
16. C. A. Owen and E. J. Campbell. The cell biology of leukocyte-mediated proteolysis. *J. Leukoc. Biol.* **65**:137–150 (1999).
17. I. A. J. M. Bakker-Woudenberg, J. C. van den Berg, and M. F. Michel. Therapeutic activities of cefazolin, cefotaxime, and ceftazidime against experimentally induced Klebsiella pneumoniae pneumonia in rats. *Antimicrob. Agents Chemother.* **22**:1042–1050 (1982).
18. A. C. Leenders, S. de Marie, M. T. ten Kate, I. A. J. M. Bakker-Woudenberg, and H. A. Verbrugh. Liposomal amphotericin B (AmBisome) reduces dissemination of infection as compared with amphotericin B deoxycholate (Fungizone) in a rate model of pulmonary aspergillosis. *J. Antimicrob. Chemother.* **38**:215–25 (1996).
19. A. Gabizon, J. Huberty, R. M. Straubinger, and D. Papahadjopoulos. An improved method for *in vivo* tracing and imaging of liposomes using a gallium 67-deferoxamine complex. *J. Lip. Res.* **1**:123–135 (1988).
20. G. R. J. Bartlett. Phosphorus assay in column chromatography. *J. Biol. Chem.* **234**:466 (1959).
21. W. Zhang, L. Guo, J. A. Nadel, and D. Papahadjopoulos. Inhibition of tracheal vascular extravasation by liposome-encapsulated albuterol in rats. *Pharm. Res.* **15**:455–460 (1998).
22. G. Thurston, T. J. Murphy, P. Baluk, J. R. Lindsey, and D. McDonald. Angiogenesis in mice with chronic airway inflammation: strain-dependent differences. *Am. J. Path.* **153**:1099–1112 (1998).
23. T. Nagase, E. Ohga, and E. Sudo. Intercellular adhesion molecule-1 mediates acid aspiration-induced lung injury. *Am. J. Resp. Crit. Care Med.* **154**:504–510 (1996).
24. J. Kurantsin-Mills, H. M. Jacobs, R. Siegel, M. M. Cassidy, and L. S. Lessin. Indium-111 oxine labeled erythrocytes: Cellular distribution and efflux kinetics of the label. *Int. J. Rad. Appl. Instr. B* **16**:821–827 (1989).
25. T. Daemen, M. Velinova, and J. Regts. Different intrahepatic distribution of phosphatidylglycerol and phosphatidylserine liposomes in the rat. *Hepatology* **26**:416–423 (1997).
26. J. Tamaoki, E. Tagaya, I. Yamawaki, N. Sakai, A. Nagai, and K. Konno. Effect of erythromycin on endotoxin-induced microvascular leakage in the rat trachea and lungs. *Am. J. Resp. Crit. Care Med.* **151**:1582–1588 (1995).
27. E. T. Dams, M. J. Becker, W. J. Oyen, O. C. Boerman, G. Storm, P. Laverman, S. de Marie, J. W. van der Meer, I. A. J. M. Bakker-Woudenberg, F. H. Corstens. Scintigraphic imaging of bacterial and fungal infection in granulocytopenic rats. *J. Nucl. Med.* **40**:2066–2072 (1999).
28. B. A. Collin and R. Ramphal. Pneumonia in the compromised host including cancer patients and transplant patients. *Inf. Dis. Clin. N. Am.* **12**:781–805 (1998).
29. S. K. Huang, F. J. Martin, G. Jay, J. Vogel, D. Papahadjopoulos, and D. S. Friend. Extravasation and transcytosis of liposomes in Kaposi's sarcoma-like dermal lesions of transgenic mice bearing the HIV tat gene. *Am. J. Path.* **143**:10–14 (1993).
30. J. Rosenecker, W. Zhang, and K. Hong. Increased liposome extravasation in selected tissues: effect of substance P. *Proc. Natl. Acad. Sci. USA* **93**:7236–7241 (1996).
31. S. K. Huang, F. J. Martin, D. S. Friend, and D. Papahadjopoulos. Mechanism of stealth liposome accumulation in some pathological tissues. In D. Lasic and F. J. Martin (eds.), *Stealth Liposomes*, CRC press, Boca Raton, 1995 pp. 119–125.